



Synthesis, characterization, and olefin (co)polymerization behavior of unsymmetrical α -diimine palladium complexes containing bulky substituents at 4-position of aniline moieties

Lihua Guo^{a,*}, Yanlan Liu^a, Wenting Sun^a, Qing Du^a, Yuliang Yang^a, Wenyu Kong^{a,b}, Zhe Liu^{a,**}, Darui Chen^{b,***}

^a School of Chemistry and Chemical Engineering, Qufu Normal University, Qufu, 273165, China

^b Key Laboratory of Polymeric Composite & Functional Materials of Ministry of Education, Sun Yat-Sen University, Guangzhou, 510275, China

ARTICLE INFO

Article history:

Received 26 June 2018

Received in revised form

1 September 2018

Accepted 19 September 2018

Available online 20 September 2018

ABSTRACT

Three novel unsymmetrical α -diimine Pd(II) complexes containing bulky substituents at 4-position of aniline moieties were prepared and characterized. Unfortunately, the introduction of large substituents on *para*-N-aryl moieties did not slow the exchange between the *anti* and *syn* forms for these complexes. These unsymmetrical α -diimine Pd(II) complexes also did not improve thermal stability and broaden molecular weight distribution in ethylene polymerization. However, these α -diimine palladium catalysts could copolymerize ethylene with biorenewable comonomer acrylic acid (AA), with comonomer incorporation in the range of 1.1–2.7% and high copolymer molecular weights. The AA units are incorporated predominately at the end of the branches. In addition, a systematic investigation on the polymerization of 1-hexene, 1-octene and 1-decene using these complexes was also performed. Changes in the ligand sterics and monomer length can influence the branch density and molecular weight of poly(α -olefins). Interestingly, these α -olefin polymers show properties characteristic of thermoplastic elastomers, i.e., good elastomeric recovery and high strain at break. Previous work has shown that ethylene or α -olefin polymerization using some nickel α -diimine catalysts can generate elastic polyolefin materials. This work may provide an alternative and effective strategy to synthesize thermoplastic elastomers by α -diimine Pd(II) catalysts in one step using only α -olefin as the feedstock.

© 2018 Elsevier B.V. All rights reserved.

1. Introduction

Since Brookhart's reported initially on Ni(II) and Pd(II) α -diimine catalysts for olefin polymerization in 1995 [1,2], substantial efforts have been devoted to this field in developing the novel late transition metal catalysts [3–20]. The big advantages of these catalysts are that they can produce polyolefins with various types of branches and have good tolerance toward polar groups [21–23]. The bulky ortho-aryl substituents in the α -diimine ligand, which could retard the chain transfer process and catalyst deactivation, is essential to achieve the high polymerization activity and high

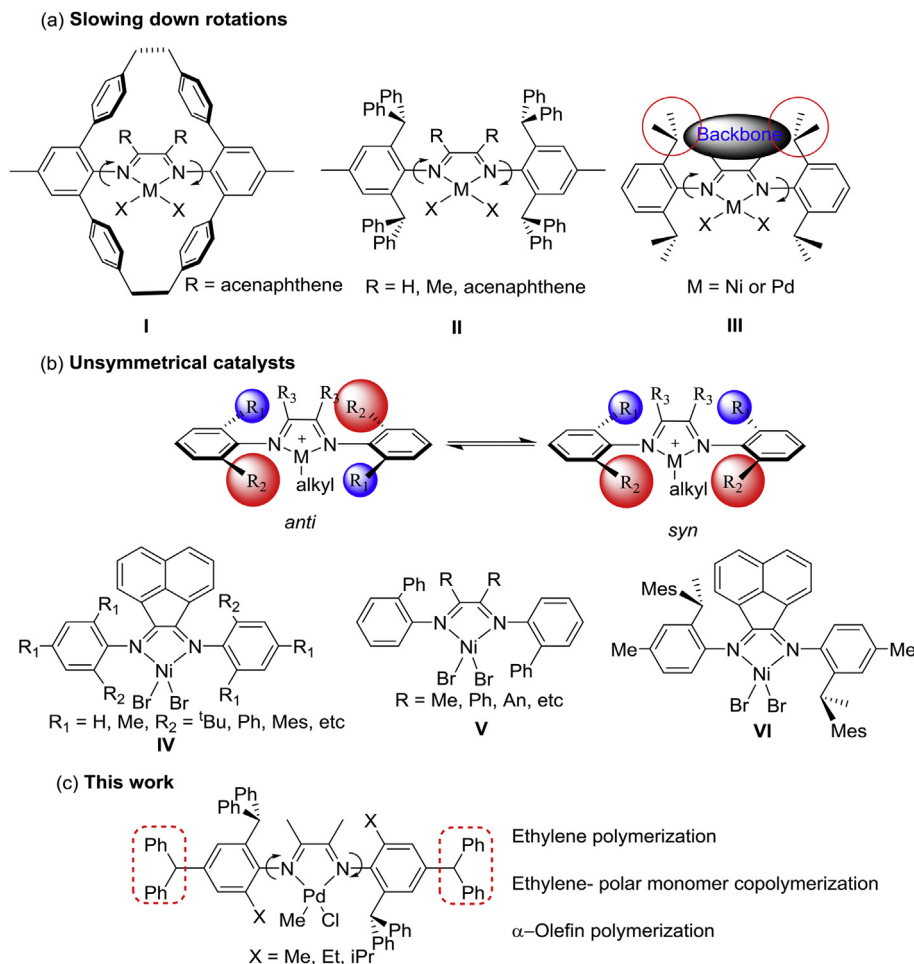
* Corresponding author.

** Corresponding author.

*** Corresponding author.

E-mail addresses: guolihua@qfnu.edu.cn (L. Guo), liuzheqd@163.com (Z. Liu), daruichen@foxmail.com (D. Chen).

polymer molecular weight. However, conventional α -diimine Ni(II) and Pd(II) catalysts suffer from the significant decrease of activity and polymer molecular weight at elevated temperatures [9,10]. Brookhart and co-workers have shown that increasing N-aryl rotations from perpendicular to square-planar coordination plane results in increased associative chain transfer and the potential decomposition arising from C-H activation of the metal center to the alkyl groups on the α -diimine ligand [24]. Thus, increasing of the steric bulk on the *o*-aryl substituents and the ligand backbone can enhance the thermal stability of these catalysts. For example, Guan et al. reported the Pd(II) α -diimine catalysts bearing a cyclophane ligand moiety (Scheme 1, I) showed the rises of thermal stability for ethylene polymerization and incorporation of methyl acrylate (MA) for copolymerization of ethylene and MA [25,26]. The Long, Chen and Sun groups developed a series of α -diimine Ni(II) and Pd(II) catalysts containing bulky dibenzhydryl (CHPh₂) moiety (Scheme 1, II), which can suppress the chain transfer and catalyst deactivation at temperature ranges suitable for industrial process



Scheme 1. (a) The strategy to slow down C-N bond rotations; (b) Interconversion between the syn- and anti-forms for unsymmetrical α -diimine metal catalyst and some previously reported examples. (c) Our current work.

(typically 80–100 °C) [27–34]. The Gao group also provided an alternative strategy by increasing the steric bulk of the α -diimine backbone for enhancing the thermal stability of Ni(II) and Pd(II) catalysts (Scheme 1, III) [35–38]. The bulk of the backbone is expected to inhibit the N-aryl rotation of the α -diimine ligand because of the repulsive interaction. The above-mentioned studies clearly indicate that the inhibition of N-aryl rotation plays an important role in enhancing the thermal stability of the catalyst and increasing the molecular weight of the polyolefins.

Moreover, a great deal of work has been focused on unsymmetrical α -diimine catalyst precursors due to their behavior of stereo-controlled olefin polymerization and the formation of bimodal polyethylene [39–45]. Unsymmetrical α -diimine metal complexes, which contain two different ortho substituents on each ring, may exist as syn- and anti-conformers (Scheme 1). The syn- and anti-conformers may exhibit different behavior in olefin polymerization. The interconversion between the syn- and anti-conformers depends strongly on the steric bulkiness of the ortho substituents of the aryl ring. When the ortho substituent are bulk enough, the interconversion through the N-aryl rotation would become very slow at room temperature. For example, the syn- and anti-conformers of Ni(II) α -diimine catalysts were isolated by Pellicchia et al. and used for propylene polymerization at –45 °C (Scheme 1, IV). The propylene produced by the syn-conformer was syndiotactic while the propylene produced by the anti-conformer showed low stereoregularity [30]. In addition, Wu group reported

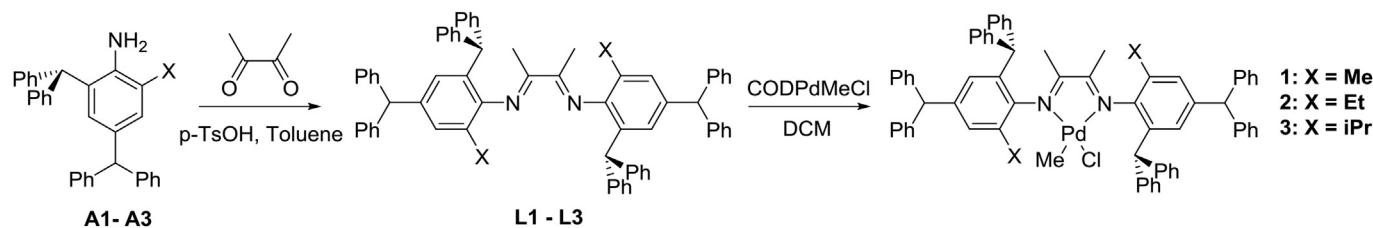
that bimodal molecular distributions may arise in ethylene polymerizations by some unsymmetrical Ni(II) α -diimine catalysts due to the slow interconversion between the syn- and anti-conformers (Scheme 1, V) [31]. The Coates group found that some bulky substituted α -diimine Ni(II) catalysts adopt exclusively anti conformations and can produce isotactic propylene at low temperature (Scheme 1, VI) [32]. These studies are mainly concentrated on the nickel catalyst. The work on the properties of unsymmetrical α -diimine Pd(II) catalysts for olefin polymerization is rarely ever done [46].

Herein, we report the synthesis of a series of novel unsymmetrical α -diimine Pd(II) complexes containing bulky substituents at 4-position of aniline moieties and the influence of the bulky ortho- and para-aryl substituents on catalytic properties in olefin polymerization and copolymerization with polar monomers.

2. Results and discussion

2.1. Synthesis of the ligands and Pd(II) complexes

The preparation of ligands **L1–L3** and corresponding palladium complexes **1–3** are shown in Scheme 2. Acid-catalyzed condensation reactions of anilines with 2,3-butanedione in toluene readily produced para-diphenylmethyl substituted α -diimine ligands in 76–85% yields. These ligands were characterized by ^1H , ^{13}C NMR and mass spectrometry. The ^1H NMR spectrum of ligand **L1** shows



Scheme 2. Synthesis of the ligands and Pd(II) complexes.

the presence of three isomers in the molar ratio of 1:5:24 (see supplementary materials, Fig. S7). The origin of the isomers may be imine C=N bond *Z,E*-isomerism and conformational *anti/syn* isomerism, which was similar to previous observation with related α -diimine ligands [22,39,41,47]. Treatments of (COD)PdMeCl (COD = 1,5-Cyclooctadiene) with the corresponding ligands in CH_2Cl_2 afforded the palladium complexes **1–3** in 57–72% yields. The palladium complexes were characterized by ^1H , ^{13}C NMR, mass spectrometry and elemental analysis. Only one Pd–Me signal and one set of chemical resonances was observed in the ^1H NMR at 60 °C and –80 °C for complexes **1–3** (see supplementary materials, Figs. S15–S16). This suggested that no isomerization occurs on the NMR time scale. However, we are unable to provide a rationale that whether only one rotamer is present or that *syn/anti* interconversion (N-aryl group rotation) is too fast. It is reasonable to assume that the fast exchange between the *syn* (with both methyl substituents on the same side of the N–Pd–N plane) and *anti* (with both methyl substituents on the opposite side of the N–Pd–N plane) isomers exists in solution, since narrow molecular weight distributions were observed for these Pd(II) complexes in ethylene polymerization. Notably, a similar behavior has been reported for analogous Pd(II) complexes [46].

Single crystal of complex **1** suitable for X-ray diffraction analysis was obtained by layering the *n*-hexane to the CH_2Cl_2 solution at room temperature (Fig. 1). As expected, the Pd center adopts a square planar geometry in the solid state. The observed bond angles and lengths are typical for previously reported palladium α -diimine complexes. In addition, a C_2 configuration, i.e. *rac* form was observed for complex **1** in the solid state. Both phenyl rings attached on imine groups are nearly perpendicular to the coordination plane, with the dihedral angles being 84.9°.

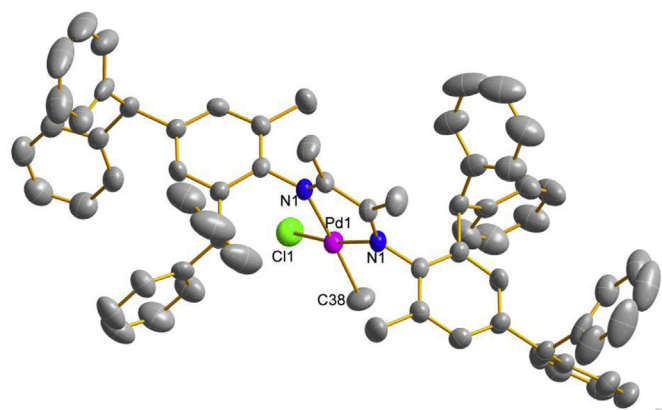


Fig. 1. Molecular structure of complex **1**. Thermal ellipsoids are shown at the 50% probability level. Hydrogen atoms have been omitted for clarity. The chlorine group and methyl group attached to Pd1 are disordered over two sites, only one orientation is shown here. Selected bond lengths (Å) and angles (deg): Pd(1)–C(38) = 2.007(18), Pd(1)–N(1) = 2.101(2), Pd(1)–Cl(1) = 2.288(4), C(38)–Pd(1)–Cl(1) = 87.3(6), N(1)–Pd(1)–N(1) = 77.29(14).

2.2. Olefin polymerization results

Ethylene polymerization was investigated by an in situ activation of the palladium complexes with 1.5 equiv. of sodium tetrakis(3,5-bis(trifluoromethyl)phenyl)borate (NaBAF). Results are summarized in Table 1. The ethylene polymerization activities and the molecular weight of the generated polyethylene decreased when the polymerization temperature was increased from 25 to 55 °C. Additionally, polymerizations conducted by complex **1** at 55 °C showed a decrease of activity from $4.1 \times 10^4 \text{ g mol}^{-1} \text{ h}^{-1}$ to $0.6 \times 10^4 \text{ g mol}^{-1} \text{ h}^{-1}$ with time (see supplementary materials, Fig. S30). These results suggest that complex **1** became unstable and the chain transfer was also enhanced at high temperatures. Further, increase in the bulk of the ortho substituents resulted in increased activities and the molecular weight of polymers, which was consistent with previous observations [1,2,4]. All of the polyethylenes prepared using these palladium catalysts are highly branched with a branching density in a narrow range of 57–67 branches per 1000 carbons, which is much lower than those by classic Brookhart catalyst (ca. 100/1000C) [1,2]. As a result, the polymer branching number is largely independent of polymerization temperature and the catalyst structures, following the same trend as some reported α -diimine Pd(II) catalysts [2–4,6]. It should be noted that Chen et al. have reported a series of α -diimine Pd(II) catalysts bearing both the dibenzhydryl moiety and systematically varied ligand sterics and achieved the tuning of the branching densities of polyethylenes though careful ligand sterics modifications [33]. Very interestingly, in contrast to the reported unsymmetrical α -diimine Ni(II) catalysts [39,41,42,45], which generated the polyethylenes with broad even bimodal molecular weight distributions, the Pd(II) catalysts in this system produced narrow molecular weight distributions (less than 2.1). This result may be attributed to two factors. First, the fast interconversion of *syn*- and *anti*-conformers would be maintained in the cationic Pd(II) species

Table 1
Ethylene polymerization with complexes **1–3**.^a

Ent.	Cat.	T (°C)	Yield (g)	Act. ^b	M_n^c (10^4)	PDI ^c	B^d
1	1	25	2.55	2.55	12.3	1.87	57
2	1	40	1.85	1.85	9.3	1.71	62
3	1	55	1.20	1.20	1.2	2.09	66
4	2	25	2.63	2.63	18.7	1.61	62
5	2	40	2.55	2.55	11.0	2.01	63
6	2	55	1.14	1.14	1.4	2.12	67
7	3	25	4.35	4.35	33.3	1.45	62
8	3	40	3.82	3.82	17.8	1.84	63
9	3	55	2.00	2.00	7.1	1.75	66

^a Polymerization conditions: 10 μmol pre-catalyst; 1.5 eq. NaBAF; 50 mL of toluene; ethylene pressure, 1.8 atm; reaction time, 10 h.

^b Activity is in unit of $10^4 \text{ g mol}^{-1} \text{ h}^{-1}$.

^c Determined by GPC using universal calibration.

^d B = branches per 1000 carbons, Branching numbers were determined using ^1H NMR spectroscopy.

during polymerization. The introduction of large substituents at 4-position of aniline moiety did not slow this exchange through the inhibition of C–N bond rotation. Second, the syn- and anti-forms of the cationic Pd(II) species may show the similar catalytic properties in ethylene polymerization.

One notable feature of α -diimine Pd(II) catalysts is their good copolymerization ability for ethylene with polar monomers. Two inexpensive and widely used monomers including methyl acrylate (MA) and AA (acrylic acid) were chosen to copolymerize with ethylene. The copolymerization results are shown in Table 2. Copolymers with high molecular weight were generated. In addition, MA and AA incorporation ratios of 1.0–4.7% for complexes **1–3** were observed. When the steric hindrance of the ortho substituents increased, the MA and AA incorporation ratio decreased. A lot of studies on ethylene/MA copolymerization using α -diimine Pd(II) catalysts have been reported [2–4,6]. The ^1H NMR spectra of the copolymers suggest that the MA units are located at the end of the branches, which result the fast chain walking after ethylene insertion [21]. However, to our knowledge, very few α -diimine Pd(II) catalysts have been reported to catalyze olefin copolymerization with biorenewable comonomer acrylic acid, particularly because of the poisoning of the metal centers by the active proton in $-\text{COOH}$. Jordan and co-workers described ethylene/AA copolymerization behavior of a series of (N,N'-diaryl- α -diimine) Pd(II) catalysts that contain bulky diarylmethyl moiety in one N-aryl rings and secondary amide ($-\text{CONHMe}$) or tertiary amide ($-\text{CONMe}_2$) groups on the other N-aryl rings [48]. However, by using the highly sterically hindered α -diimine Pd(II) catalysts containing naphthalene or benzothiophene units on both N-aryl rings, no AA incorporation was observed in ethylene-AA copolymerization [30]. As a result, the ability of the unsymmetrical α -diimine Pd(II) catalysts in this system to copolymerize ethylene with AA may be attributed to the right steric hindrance of the unsymmetrical ligands, which can narrow the gap in the insertion barriers between ethylene and AA.

The ^1H NMR and ^{13}C NMR spectra of the ethylene/AA copolymer indicate the incorporation of the AA monomer (Fig. 2 and Figs. S44–47 in supplementary materials). The AA radical homopolymer is insoluble in CDCl_3 , while the ethylene/AA copolymer is soluble. The characteristic peak for AA homopolymer generated via radical polymerization was at ca. δ 2.38 in CD_3OH , corresponding to $-\text{CH}_2\text{CH}(\text{COOH})$, and was very broad because of the irregularity of the repeating units [32]. This peak was not observed in the ^1H NMR of ethylene/AA copolymer. These results suggested that no AA radical homopolymerization occurred. The triplet at 2.34 ppm was assigned to the methylene hydrogen of the $-\text{CH}_2\text{COOH}$ moiety. The AA units are incorporated predominately at the end of the

branches, which is similar to the case of ethylene/MA copolymerization and ethylene/AA copolymers reported by Jordan group [47].

The 1-hexene, 1-octene and 1-decene polymerizations were also investigated and the results were summarized in Table 3. The TOF increased with decreasing the bulk of the *ortho*-substituents in the order of **1** > **2** > **3**. The sterically bulky substituents may retard the coordination and insertion of α -olefins. In contrast to the trend of TOF, the molecular weight of the obtained polymers was slightly increased with the increasing the bulk of the ortho-substituents (e.g. Table 3, Entries 1–3). This is probably due to the suppression of the chain transfer by sterically blocking the access of the monomer to the axial positions of the metal coordination site. ^1H NMR spectroscopy analysis showed that all the resulting polymers were much lower branched than predicated from regular and exclusive 1,2-monomer enchainment, i.e. 167 branches/1000C for poly(1-hexene), 125 branches/1000C for poly(1-octene), 100 branches/1000C for poly(1-decene) (Scheme 3, regioregular polymer). This is due to a fraction of 2,1 insertion followed by chain walking to the primary carbon (Scheme 3, 1, ω -enchainment). As a result, “chain straightening” through 1, ω -enchainment leads to a more linear polymer structure. The fraction of 1, ω -enchainment ranged from 42 to 54% and was comparable to the classical Brookhart catalyst [49], thus indicating that this class of complexes did not have a significant selectivity for insertion fashion (1,2- vs 2,1-insertion) of α -olefins. Specially, increasing the steric bulk of the ligand from the *ortho*-methyl to *ortho*-isopropyl substituents resulted in a lower branched polymer with higher degree of 1, ω -enchainment. When monomer length increases from C6 to C10, the fraction of 1, ω -enchainment for 1-hexene, 1-octene and 1-decene is slightly changed. However, the branching density could be dramatically reduced from 91 to 109 branches/1000C to 51–66 branches/1000C. This difference in branching density translated into greater differences in polymer melting points (11–16 °C versus 57–59 °C). Most interestingly, the microstructure analysis of poly(1-hexene) based on ^{13}C NMR spectroscopy showed the presence of only methyl, butyl, and long chain branches (\geq hexyl) for all the catalysts (Fig. 3a). In addition, poly(1-octene) and poly(1-decene) made with these catalysts showed only methyl and long chain branches (\geq hexyl) (Fig. 3b and c). The typical peaks of methyl (1B_1 at ca. 19.9 ppm) and long chain branches (1B_{6+} at ca. 14.3 ppm and 2B_{6+} at ca. 22.9 ppm) can be safely identified in the ^{13}C NMR spectra. No ethyl, propyl, or adjacent methyl branches were detectable, indicating that the insertion occurred only into primary Pd-alkyl bonds.

The mechanical properties of these poly(α -olefins) were examined by tensile tests (Fig. 4). The product generated from 1-hexene and 1-octene polymerization showed very low stress at break values. For comparison, poly(1-decene) sample showed high stress and strain at break values (6.27 Mpa and 1340%). These results are attributed to longer methylene sequences in the 1-decene polymer backbone. Clearly, the polymer microstructures including molecular weights and branching densities, which can be modulated by monomer length, have a significant influence on the mechanical properties of these polymers.

The elastic recovery, i.e., the capability to return to the initial state once the force is removed was also investigated (Fig. 5). Polymer samples were subjected to hysteresis testing where each sample was extended to 300% strain over 10 cycles. The strain recovery values (SR) can be calculated by $\text{SR} = 100 (\epsilon_a - \epsilon_r) / \epsilon_a$, where ϵ_a is the applied strain and ϵ_r is the strain in the cycle at zero load after 10th cycle. These polymer samples exhibit a certain amount of unrecovered strain after the first cycle, followed by minimal deformation on each subsequent cycle. A permanent structural change happens during the first cycle, after which better elastomeric properties are created. The elastic recovery behavior of 1-

Table 2
Ethylene-polar monomer copolymerization with complexes **1–3**.^a

Ent.	Cat.	Monomer	X^b (%)	Yield (g)	Act. ^c	M_n^d (10^4)	PDI ^d	B^e
1	1	MA	4.7	0.39	10.83	1.0	1.52	50
2	2	MA	3.4	0.52	14.44	1.2	1.53	60
3	3	MA	1.0	0.57	15.83	1.4	1.58	60
4	1	AA	2.7	0.83	23.06	1.8	1.80	53
5	2	AA	2.2	0.94	26.11	3.3	1.45	55
6	3	AA	1.1	1.24	34.44	5.8	1.48	62

^a Conditions: total volume of CH_2Cl_2 and polar vinyl monomer, 50 mL; 30 μmol pre-catalyst; 1.5 eq. NaBAF; polar monomer concentration, 1 M; ethylene pressure, 1.8 atm; reaction time, 12 h; reaction temperature, 30 °C.

^b Determined by ^1H NMR spectroscopy.

^c Activity is in unit of $10^2 \text{ g mol}^{-1} \text{ h}^{-1}$.

^d Determined by GPC using universal calibration.

^e B = branches per 1000 carbons, Branching numbers were determined using ^1H NMR spectroscopy.

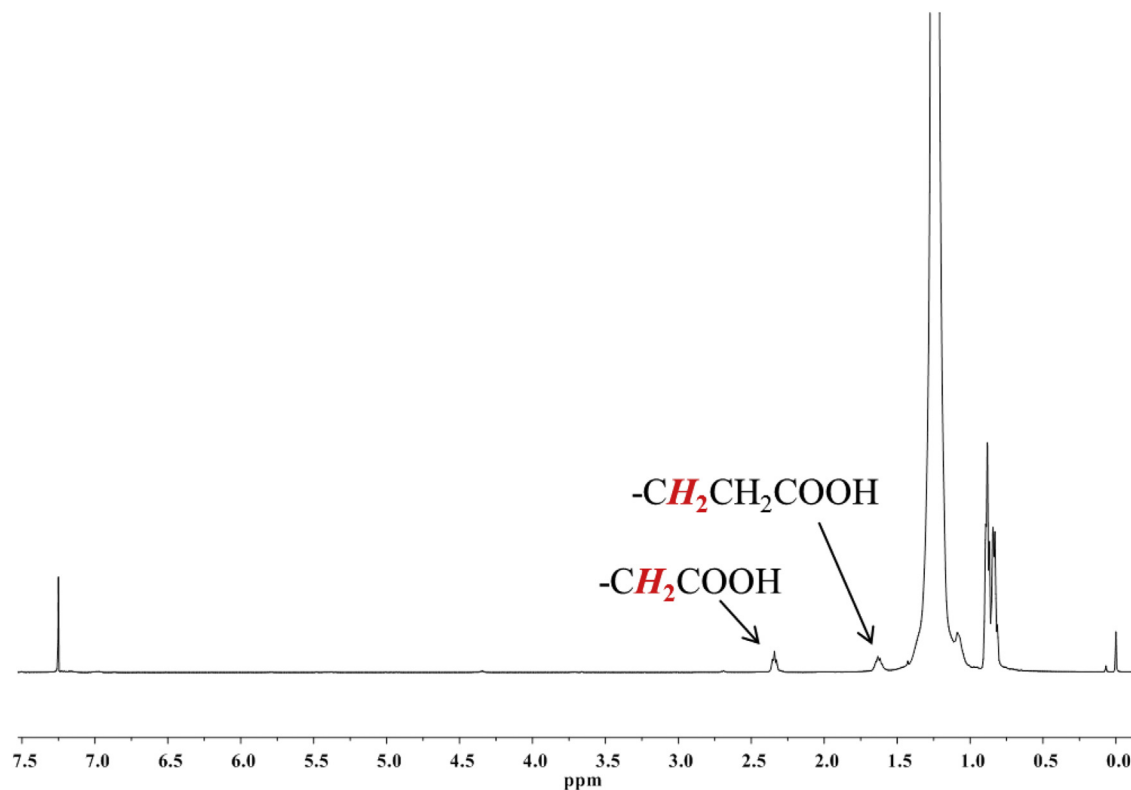


Fig. 2. ^1H NMR spectra of the ethylene-AA copolymer obtained by complex **3** (CDCl_3 , sample from Table 2, entry 6).

Table 3
 α -olefin polymerization with complexes **1–3**.^a

Ent.	Cat.	[M]	Yield (g)	TOF ^b (h^{-1})	M_n^c (10^4)	PDI ^c	B ^d	$1,\omega^e$ (%)	T_m^f ($^\circ\text{C}$)
1	1	1-Hexene	4.01	159	14.4	1.88	109	46	15
2	2	1-Hexene	3.24	128	14.7	1.68	101	50	16
3	3	1-Hexene	2.66	105	15.2	1.60	91	54	11
4	1	1-Octene	2.10	62	6.7	1.90	76	47	35
5	2	1-Octene	1.70	51	7.6	1.90	72	50	36
6	3	1-Octene	1.68	50	8.0	1.99	69	51	31
7	1	1-Decene	3.34	79	10.8	1.82	66	42	57
8	2	1-Decene	2.50	59	11.0	1.89	64	43	59
9	3	1-Decene	2.30	55	13.1	1.69	51	54	58

^a Polymerization conditions: total volume of toluene and monomer, 50 mL; monomer concentration, 3 M; 30 μmol pre-catalyst; 1.5 eq. NaBAF; reaction temperature, 25 $^\circ\text{C}$, reaction time, 10 h.

^b Turnover frequency = moles of substrate converted per mole of catalyst per hour.

^c Determined by GPC using universal calibration.

^d B = branches per 1000 carbons, Branching numbers were determined using ^1H NMR spectroscopy.

^e $1,\omega$ -enchainment calculated from the equation according to reference [49]: % $1,\omega = [(1000 - (n-2)B)/(1000 + 2B)] \times 100$, R stands for the total methyl groups per 1000 methylene groups, n stands for the monomer length, i.e. the carbon atom number of monomer.

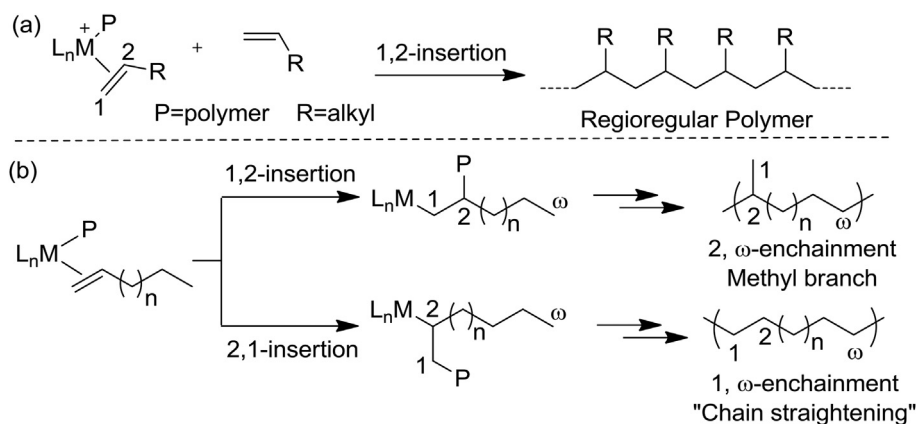
^f Determined by differential scanning calorimeter (DSC).

hexene polymer was not determined due to its very low strain at break values. Overall, monomer length plays an important role on the elastic properties of these polymer samples. The unrecovered strain from 300% after 10th cycle is 159% for the polymer sample produced using 1-octene as monomer (SR = 47%), while higher unrecovered strain (208%) is observed for the polymer sample produced using 1-decene as monomer (SR = 31%). This trend is opposite to the effect of monomer length on stress and strain at

break values. These samples exhibit high SR values, which are comparable with previously reported elastic polyolefin materials obtained by reported nickel α -diimine catalysts [43,50–55]. As a result, α -olefin polymerization in this system can generate thermoplastic elastomers with good elastomeric recovery and high strain at break. The current palladium catalytic system may provide a rare route to the synthesis of thermoplastic elastomers in one step using only α -olefin as the feedstock [53,56].

3. Conclusions

In summary, three unsymmetrical α -diimine palladium complexes containing bulky substituents at 4-position of aniline moieties were synthesized and characterized. The aim was to investigate the effect of bulky substituents at 4-position of aniline moieties on the polymerization processes as well as the properties of the resulting polymer products. The Pd(II) catalysts in this system produced polyethylenes with narrow molecular weight distributions (less than 2.1). The introduction of large substituents on *para*-N-aryl moieties did not slow the exchange between the *anti* and *syn* forms for these complexes. However, these α -diimine palladium catalysts could copolymerize ethylene with bio-renewable comonomer acrylic acid, with high comonomer incorporation and high copolymer molecular weights and the AA units are incorporated predominately at the end of the branches. In addition, the polymerization behavior of higher α -olefins using these catalysts was also investigated. The tuning in ligand sterics and monomer length enables the tuning of the polymer microstructures such as branching density through the fraction of $1,\omega$ -enchainment. The most abundant branches of these polymers are methyl and longer than butyl branches. Interestingly, these poly(α -olefins) catalyzed by α -diimine Pd(II) catalysts in this system displayed properties characteristic of thermoplastic elastomers. Thus,



Scheme 3. Modes of monomer insertion and enchainment in Pd(II) catalyzed α -olefin polymerization.

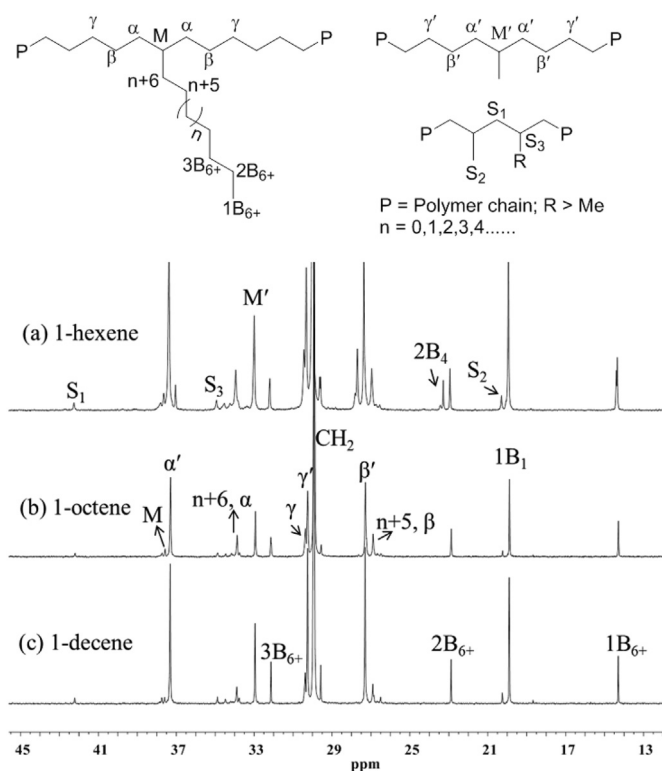


Fig. 3. ^{13}C NMR spectra of polymers of (a) 1-hexene, (b) 1-octene, (c) 1-decene polymerized by complex 1. The large peak at 30 ppm is $(CH_2)_n$. Common signals are only labeled on one of the four spectra for clarity. For example, $1B_1$, which is present in all four spectra, is only labeled in (a).

this work demonstrates the great potential of synthesizing thermoplastic elastomers by α -diimine Pd(II) catalysts in a single step using only α -olefin as the feedstock.

4. Experimental section

4.1. General procedures

Analytically pure solvent (toluene, n-hexane, dichloromethane) were dried before use. All other reagents were purchased from commercial sources and used without purification. The synthetic route for anilines **A1-A3** was shown in supporting information. 1H NMR spectra were acquired in 5 mm NMR tubes at 298 K on Bruker

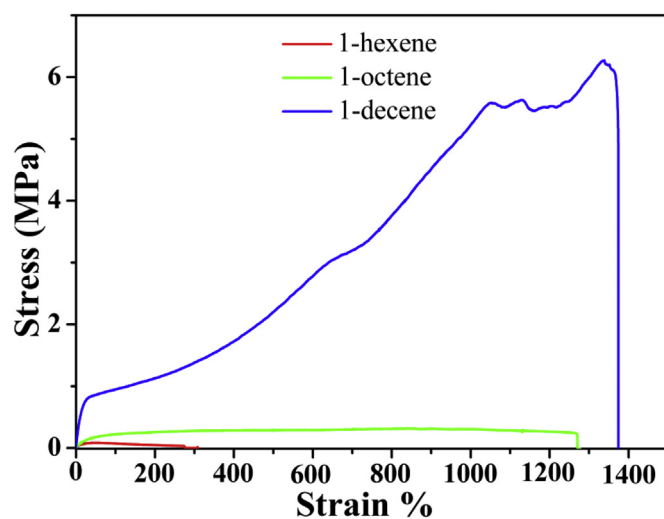


Fig. 4. Stress-strain curves for polymers generated by complex 1.

DPX 500 spectrometers using TMS as an internal standard and $CDCl_3$ as solvent. ^{13}C NMR spectra were acquired in 5 mm NMR tubes at 298 K on Bruker DPX 500 or Bruker Ascend Tm 400 spectrometers. ^{13}C NMR chemical shifts were internally referenced to $CHCl_3$ (77.16 ppm) for chloroform- d_1 . Elemental analyses were performed on a Vario EL microanalyzer. Mass spectra were obtained using electro spray ionization (ESI) LCMS-2010A for the anilines and **L1-L3**. Matrix assisted laser desorption ionization time of flight mass (MALDI-TOF) were performed on Bruker ultrafleXtreme for complexes **1-3**. The molecular weight and the molecular weight distribution of the polymers were determined by gel permeation chromatography (GPC, Tosh, Tokyo, Japan) equipped with two linear Styragel columns at 40 °C using THF as a solvent and calibrated with polystyrene standards, and THF was employed as the eluent at a flow rate of 0.35 mL/min. At least three specimens of each polymer were tested. DSC was performed by a DSC Q20 from TA Instruments. Samples were quickly heated to 100 °C and kept for 5 min to remove thermal history, then cooled to -70 °C at a rate of 10 K/min, and finally reheated to 100 °C at the same rate under a nitrogen flow (50 mL/min). The maximum points endotherm (heating scan) were taken as the melting temperature (T_m). Stress/strain experiments were performed at 10 mm/min by means of a Universal Test Machine (UTM2502) at room temperature. Polymers were melt-pressed at 30–35 °C above their melting point

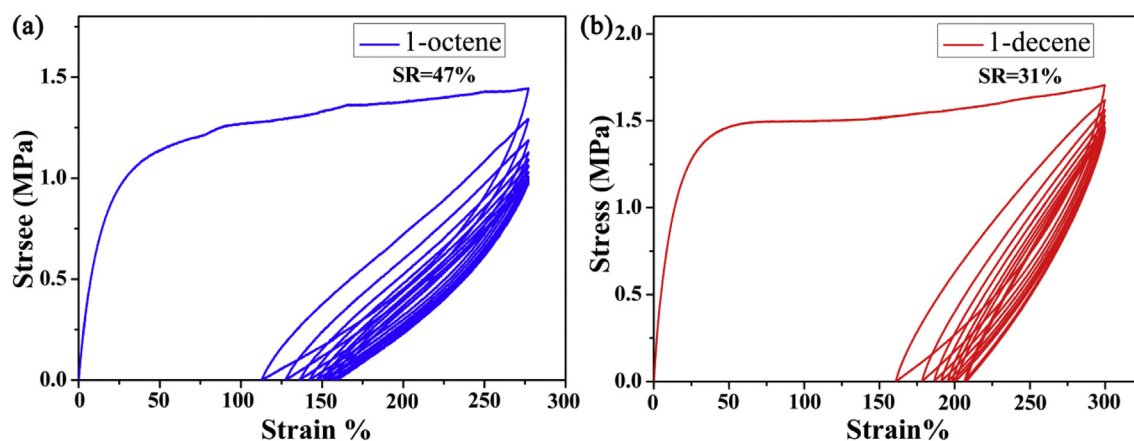


Fig. 5. Plots of hysteresis experiments of ten cycles at a strain of 300% for samples generated by complex 1, (a) 1-octene (Table 3, entry 4) (b) 1-decene (Table 3, entry 7).

to obtain the test specimens, which have 14-mm gauge length, 2-mm width, and thickness of 0.5 mm.

4.2. Synthesis of ligands

4.2.1. Preparation of **L1**

A solution of **A1** (3.8 g, 8.6 mmol), 2,3-butadione (0.37 g, 4.3 mmol) and p-toluenesulfonic acid (20 mg) in toluene (50 mL) was stirred at 80 °C until there was one main point on the TLC plate. The solvent was partially evaporated under reduced pressure until the formation of a yellow solid. The yellow solid was filtered, washed three times by 20 mL methanol and dried under high vacuum. A amount of the product (3.02 g) was obtained as yellow powder in 75.6% yield. ¹H NMR (500 MHz, CDCl₃) three isomers. isomer 1: isomer 2: isomer 3 = 1:5:24 (molar ratio), δ 7.22–6.89 (m, 40H, Ar-H), 6.83 (d, *J* = 15.3 Hz, 2H, Ar-H), 6.57 (d, *J* = 35.0 Hz, 2H, Ar-H), 5.38 (s, 2H, CHPh₂), 5.27 (s, 2H, CHPh₂), isomer 1: 2.50 (s, 0.2H, CH₃), isomer 3: 1.91 (s, 4.8H, CH₃), isomer 2: 1.86 (s, 1H, CH₃), isomer 2: 1.57 (s, 1H, N=CMe), isomer 3: 1.28 (s, 4.8H, N=CMe), isomer 1: 1.11 (s, 0.2H, N=CMe). ¹³C NMR (126 MHz, CDCl₃) δ 168.98 (N=CMe), 146.26, 144.35, 143.42, 142.55, 138.35, 132.73, 129.67, 129.39, 128.86, 128.52, 128.22, 128.02, 126.15, 124.18, 56.35 (CHPh₂), 53.46 (CHPh₂), 52.50 (CHPh₂), 51.91 (CHPh₂), 18.07 (CH₃), 17.95 (CH₃), 16.38 (N=CMe), 15.85 (N=CMe). ESI-MS (*m/z*): calcd for C₇₀H₆₁N₂: 929.4835, found: 929.4827 [M+H]⁺.

4.3. Preparation of **L2**

The same procedure as above was employed. Yield 84.9% (3.49 g, yellow powder). ¹H NMR (500 MHz, CDCl₃) two isomers. isomer 1: isomer 2 = 1:5 (molar ratio), δ 7.22–6.86 (m, 42H, Ar-H), 6.53 (s, 2H, Ar-H), 5.40 (s, 2H, CHPh₂), 5.25 (s, 2H, CHPh₂), 2.21 (ddt, *J* = 22.3, 15.0, 7.5 Hz, 4H, CH₂), isomer 1: 1.56 (s, 1H, N=CMe), isomer 2: 1.29 (s, 5H, N=CMe), isomer 2: 1.12 (t, *J* = 7.5 Hz, 5H, CH₃), isomer 1: 1.01 (t, *J* = 7.4 Hz, 1H, CH₃). ¹³C NMR (126 MHz, CDCl₃) δ 169.02 (N=CMe), 145.78, 144.55, 143.67, 142.59, 138.37, 132.18, 129.69, 129.43, 128.50, 128.22, 128.03, 127.40, 126.16, 56.53 (CHPh₂), 52.48 (CHPh₂), 51.93 (CHPh₂), 24.65 (CH₂), 24.03 (CH₂), 16.62 (N=CMe), 16.17 (N=CMe), 13.88 (CH₃), 13.59 (CH₃). ESI-MS (*m/z*): calcd for C₇₂H₆₅N₂: 957.5148, found: 957.5128 [M+H]⁺.

4.4. Preparation of **L3**

The same procedure as above was employed. Yield 78.7% (3.33 g, yellow powder). ¹H NMR (500 MHz, CDCl₃) two isomers. isomer 1: isomer 2 = 1:5 (molar ratio), δ 7.24–6.87 (m, 42H, Ar-H), 6.50 (d,

J = 1.6 Hz, 2H, Ar-H), 5.41 (s, 2H, CHPh₂), 5.23 (s, 2H, CHPh₂), 2.50 (m, 2H, CH(CH₃)₂), isomer 1: 1.55 (s, 1H, N=CMe), isomer 2: 1.30 (s, 5H, N=CMe), isomer 2: 1.14 (d, *J* = 6.9 Hz, 5H, CH₃), isomer 2: 1.09 (d, *J* = 6.8 Hz, 5H, CH₃), isomer 1: 1.04 (dd, *J* = 6.8, 3.3 Hz, 1H, CH₃), isomer 1: 1.01 (dd, *J* = 6.7, 1.8 Hz, 1H, CH₃). ¹³C NMR (126 MHz, CDCl₃) δ 169.14 (N=CMe), 145.05, 144.65, 143.82, 142.60, 138.38, 134.85, 131.92, 129.70, 129.43, 128.87, 128.47, 128.22, 128.01, 126.32, 126.10, 125.09, 56.64 (CHPh₂), 52.57 (CHPh₂), 52.05 (CHPh₂), 28.47 (CH(CH₃)₃), 27.85 (CH(CH₃)₃), 24.14 (CH₃), 23.21 (CH₃), 22.99 (CH₃), 22.55 (CH₃), 16.84 (N=CMe), 16.48 (N=CMe). ESI-MS (*m/z*): calcd for C₇₄H₆₉N₂: 985.5618, found: 985.5447 [M+H]⁺.

4.5. Synthesis of the palladium complexes

4.5.1. Preparation of complex **1**

A mixture of **L1** (0.93 g, 1 mmol), (COD)PdMeCl (0.27 g, 1 mmol) and CH₂Cl₂ (20 mL) was stirred for 2 days at room temperature. During stirring, the solid was completely dissolved and the color of the solution was changed from yellow to red. The solvent was removed, and the resulting powder was washed with n-hexane (3 × 10 mL) and dried under vacuum to obtain a red solid (0.70 g, 64%). A single crystal of complex **1** was obtained by layering n-hexane onto the CH₂Cl₂ solution at room temperature. ¹H NMR (500 MHz, CDCl₃) δ 7.24–6.99 (m, 38H, Ar-H), 6.95 (s, 3H, Ar-H), 6.86 (s, 1H, Ar-H), 6.66 (s, 1H, Ar-H), 6.53 (s, 1H, Ar-H), 6.15 (s, 1H, CHPh₂), 5.89 (s, 1H, CHPh₂), 5.43 (d, *J* = 10.4 Hz, 2H, CHPh₂), 2.25 (d, *J* = 9.4 Hz, 6H, N=CMe), 0.78 (s, 3H, CH₃), 0.61 (s, 3H, CH₃), 0.56 (s, 3H, Pd-CH₃). ¹³C NMR (126 MHz, CDCl₃) δ 176.69 (N=CMe), 171.61 (N=CMe), 144.24, 144.00, 143.65, 142.56, 142.34, 142.07, 141.68, 141.25, 135.73, 135.57, 130.48, 130.27, 129.77, 129.55, 129.48, 129.38, 129.34, 129.30, 129.23, 128.76, 128.33, 127.91, 126.45, 126.19, 56.25 (CHPh₂), 52.50 (CHPh₂), 52.21 (CHPh₂), 19.02 (CH₃), 18.53 (CH₃), 18.30 (N=CMe), 17.98 (N=CMe), 2.88 (Pd-CH₃). MALDI-TOF-MS (*m/z*): calcd for C₇₀H₆₀N₂Pd: 1033.3807, found: 1033.3311 [M-Me-Cl]⁺. Anal. Calcd for C₇₁H₆₃ClN₂Pd: C, 78.51; H, 5.85; N, 2.58; Found: C, 78.41; H, 5.76; N, 2.60.

4.6. Preparation of complex **2**

Using the same procedure as for the synthesis of complex **1**, complex **2** was obtained as a red powder (0.63 g, 57%). ¹H NMR (500 MHz, CDCl₃) δ 7.23–6.97 (m, 39H, Ar-H), 6.95 (d, *J* = 7.7 Hz, 2H, Ar-H), 6.91 (s, 1H, Ar-H), 6.65 (s, 1H, Ar-H), 6.52 (s, 1H, Ar-H), 6.23 (s, 1H, CHPh₂), 5.94 (s, 1H, CHPh₂), 5.45 (d, *J* = 11.3 Hz, 2H, CHPh₂), 2.77 (dd, *J* = 15.3, 7.6 Hz, 1H, CH₂), 2.64 (dd, *J* = 14.8, 7.4 Hz, 1H, CH₂), 2.37 (m, 2H, CH₂), 1.41 (t, *J* = 7.5 Hz, 3H, CH₃), 1.33 (t, *J* = 7.5 Hz, 3H, CH₃),

0.80 (s, 3H, N=CMe), 0.62 (s, 3H, N=CMe), 0.55 (s, 3H, Pd-CH₃). ¹³C NMR (126 MHz, CDCl₃) δ 176.64 (N=CMe), 171.57 (N=CMe), 144.3, 144.10, 143.76, 142.77, 142.61, 142.44, 141.83, 141.47, 141.19, 135.66, 135.39, 133.78, 132.72, 130.45, 130.21, 129.83, 129.44, 129.08, 128.78, 128.35, 127.95, 127.34, 126.81, 126.48, 126.18, 56.42 (CHPh₂), 52.65 (CHPh₂), 52.37 (CHPh₂), 24.53 (CH₂), 23.90 (CH₂), 19.51 (CH₃), 18.39 (CH₃), 14.35 (N=CMe), 13.24 (N=CMe), 3.32 (Pd-CH₃). MALDI-TOF-MS (*m/z*): calcd for C₇₂H₆₄N₂Pd: 1061.4120, found: 1061.3390, [M-Me-Cl]⁺. Anal. Calcd for C₇₃H₆₇ClN₂Pd: C, 78.69; H, 6.06; N, 2.51; Found: C, 78.42; H, 6.16; N, 2.64.

4.7. Preparation of complex 3

Using the same procedure as for the synthesis of complex 1, complex 3 was obtained as a red powder (0.82 g, 72%). ¹H NMR (500 MHz, CDCl₃) δ 7.24–7.06 (m, 28H, Ar-H), 7.05–6.98 (m, 12H, Ar-H), 6.95 (d, *J* = 7.1 Hz, 2H, Ar-H), 6.63 (s, 1H, Ar-H), 6.50 (d, *J* = 12.7 Hz, 1H, Ar-H), 6.20 (s, 1H, CHPh₂), 5.98 (s, 1H, CHPh₂), 5.45 (m, 2H, CHPh₂), 2.92 (m, 2H, CH(CH₃)₂), 1.48 (dd, *J* = 12.3, 6.7 Hz, 4H, CH₃), 1.35 (d, *J* = 6.6 Hz, 2H, CH₃), 1.21 (t, *J* = 9.2 Hz, 6H, CH₃), 0.86 (s, 3H, Pd-CH₃), 0.62 (m, 6H, N=CMe). ¹³C NMR (126 MHz, CDCl₃) δ 176.63 (N=CMe), 171.62 (N=CMe), 144.41, 144.12, 143.77, 142.82, 142.64, 141.87 (s), 141.52, 140.68, 140.43, 138.84, 137.53, 135.49, 135.31, 130.36, 130.17, 129.82, 129.57, 129.48, 129.37, 129.33, 129.30, 129.29, 128.78, 128.49, 128.41, 128.25, 127.97, 126.82, 126.48, 126.16, 125.76, 124.87, 56.49 (CHPh₂), 56.47 (CHPh₂), 52.80 (CHPh₂), 52.54 (CHPh₂), 28.43 (CH(CH₃)₂), 28.16 (CH(CH₃)₂), 24.87 (CH₃), 23.94 (CH₃), 23.54 (CH₃), 22.63 (CH₃), 20.05 (N=CMe), 18.60 (N=CMe), 3.70 (Pd-CH₃). MALDI-TOF-MS (*m/z*): calcd for C₇₄H₆₈N₂Pd: 1090.4417, found: 1090.3704, [M-Me-Cl]⁺. Anal. Calcd for C₇₅H₇₁ClN₂Pd: C, 78.86; H, 6.27; N, 2.45; Found: C, 78.88; H, 6.19; N, 2.51.

4.8. General procedure for ethylene polymerization

Polymerization was carried out in a 250 mL round-bottomed Schlenk flask. The reactor was first dried by heating at 110 °C and cooled to room temperature under vacuum. A 250 mL round-bottomed Schlenk flask was charged with the required amount of pre-catalyst (10 μmol), NaBAF (1.5 eq.), 50 mL of freshly distilled toluene and a magnetic stirrer. The Schlenk flask was connected to a high pressure polymerization line and the solution was degassed. The vessel was warmed to the set temperature by using an oil bath. With rapid stirring, the reactor was pressurized and maintained at 1.8 atm of ethylene. After 10 h, the Schlenk flask was vented and the polymer was precipitated in methanol, washed with methanol several times, and the sticky polymer was redissolved in petroleum ether. The polymer solution was filtered through alumina or silica to remove catalyst residues. After evaporation, the resulting polymer was collected and dried under vacuum at 40 °C to a constant weight. Polymer branching density was determined by ¹H NMR. $B = 1000 \times 2(I_{CH_3})/3(I_{CH_2+CH} + I_{CH_3})$ [35].

4.9. General procedure for ethylene-polar monomer copolymerization

Polymerization was carried out in a 250 mL round-bottomed Schlenk flask. The reactor was first dried by heating at 110 °C and cooled to room temperature under vacuum. A 250 mL round-bottomed Schlenk flask was charged with the required amount of pre-catalyst (30 μmol), NaBAF (1.5 eq.), freshly distilled CH₂Cl₂, polar monomer (MA or AA) and a magnetic stirrer. The total reaction volume was kept at 50 mL. The Schlenk flask was connected to a high pressure polymerization line and the solution was degassed. The vessel was warmed to 30 °C by using an oil bath. The ethylene

pressure was kept at a constant value of 1.8 atm by continuous feeding of gaseous ethylene throughout the reaction. The polymerization was terminated by the addition of a large amount of methanol after continuous stirring for 12 h. Then the methanol was decanted off, and the sticky polymer was redissolved in petroleum ether. The polymer solution was filtered through alumina or silica to remove catalyst residues. After evaporation, the resulting polymer was collected and dried under vacuum at 40 °C to a constant weight. MA or AA incorporation was determined by ¹H NMR. $MA\% = 1/3 I_{OCH_3}/[I_{OCH_3}/3 + [(I_{CH_3} + I_{CH_2+CH})-3]/4] \times 100\%$ [57]. $AA\% = 1/2 I_{\alpha-CH_2}/[I_{\alpha-CH_2}/2 + (I_{CH_3} + I_{CH_2+CH} + 1/2 I_{\alpha-CH_2})/4] \times 100\%$ [32].

4.10. General procedure for α-olefin polymerization

Polymerization was carried out in a 100 mL round-bottomed Schlenk flask. The reactor was first dried by heating at 110 °C and cooled to room temperature under vacuum. Pre-catalyst (30 μmol), NaBAF (1.5 eq.), freshly distilled toluene, monomer and a magnetic stirrer were transferred into the reactor vessel in that order. The total volume of toluene and monomer were kept at 50 mL. They were stirred for 10 h at 25 °C. Polymerization was quenched with ethanol. The solid polymer was filtered, washed with ethanol several times, and dried in vacuum at 40 °C to a constant weight.

Acknowledgements

This work was supported by Shandong Provincial Natural Science Foundation (ZR2018MB023), the National Natural Science Foundation of China (Grant No. 21671118), The Key Laboratory of Polymeric Composite & Functional Materials of Ministry of Education (PCFM-2017-01), Excellent experiment project of Qufu Normal University (jp201705) and the Taishan Scholars Program.

Appendix A. Supplementary data

Supplementary data to this article can be found online at <https://doi.org/10.1016/j.jorganchem.2018.09.016>.

References

- [1] L.K. Johnson, C.M. Killian, M. Brookhart, *J. Am. Chem. Soc.* 117 (1995) 6414–6415.
- [2] S.D. Ittel, L.K. Johnson, M. Brookhart, *Chem. Rev.* 100 (2000) 1169–1203.
- [3] A. Nakamura, S. Ito, K. Nozaki, *Chem. Rev.* 109 (2009) 5215–5244.
- [4] L.H. Guo, S.Y. Dai, X.L. Sui, C.L. Chen, *ACS Catal.* 6 (2016) 428–441.
- [5] L.H. Guo, W.J. Liu, C.L. Chen, *Mater. Chem. Front.* 1 (2017) 2487–2494.
- [6] L.H. Guo, C.L. Chen, *Sci. China Chem.* 58 (2015) 1663–1673.
- [7] S.Y. Xiong, L.H. Guo, S.M. Zhang, Z. Liu, *Chin. J. Chem.* 35 (2017) 1209–1221.
- [8] S.Y. Dai, C.L. Chen, *Macromolecules* (2018), <https://doi.org/10.1021/acs.macromol.8b01261>.
- [9] M. Chen, C.L. Chen, *Angew. Chem. Int. Ed.* 57 (2018) 3094–3098.
- [10] P.J. Ji, L.H. Guo, X.H. Hu, W.M. Li, *J. Polym. Res.* 24 (2017) 30.
- [11] L.H. Guo, X.Y. Jing, S.Y. Xiong, W.J. Liu, Y.L. Liu, Z. Liu, C.L. Chen, *Polymers* 8 (2016) 389.
- [12] W.Y. Li, L.H. Guo, W.M. Li, *Mol. Catal.* 433 (2017) 122–127.
- [13] L.H. Guo, K.B. Lian, W.Y. Kong, S. Xu, G.R. Jiang, S.Y. Dai, *Organometallics* 37 (2018) 2442–2449.
- [14] J.H. Chen, L.H. Guo, P.J. Ji, W.M. Li, *Polym. Bull.* 75 (2018) 371–380.
- [15] G.Z. Song, L.H. Guo, Q. Du, W.Y. Kong, W.M. Li, Z. Liu, *J. Organomet. Chem.* 858 (2018) 1–7.
- [16] L.H. Guo, W.Y. Kong, Y.J. Xu, Y.L. Yang, R. Ma, L. Cong, S.Y. Dai, Z. Liu, *J. Organomet. Chem.* 859 (2018) 58–67.
- [17] S.H. Zhong, Y.X. Tan, L. Zhong, J. Gao, H. Liao, L. Jiang, H.Y. Gao, Q. Wu, *Macromolecules* 50 (2017) 5661–5669.
- [18] B.K. Long, J.M. Eagan, M. Mulzer, G.W. Coates, *Angew. Chem. Int. Ed.* 55 (2016) 7106–7110.
- [19] D. Takeuchi, *Macromol. Chem. Phys.* 212 (2011) 1545–1551.
- [20] Z. Guan, P.M. Cotts, E.F. McCord, S.J. McLain, *Science* 283 (1999) 2059–2061.
- [21] L.K. Johnson, S. Mecking, M. Brookhart, *J. Am. Chem. Soc.* 118 (1996) 267–268.
- [22] S. Mecking, L.K. Johnson, L. Wang, M. Brookhart, *J. Am. Chem. Soc.* 120 (1998) 888–899.

- [23] D.P. Gates, S.A. Svejda, E. Oñate, C.M. Killian, L.K. Johnson, P.S. White, M. Brookhart, *Macromolecules* 33 (2000) 2320–2334.
- [24] D.J. Tempel, L.K. Johnson, R.L. Huff, P.S. White, M. Brookhart, *J. Am. Chem. Soc.* 122 (2000) 6686–6700.
- [25] D.H. Camacho, E.V. Salo, J.W. Ziller, Z. Guan, *Angew. Chem. Int. Ed.* 43 (2004) 1821–1825.
- [26] C.S. Popeney, D.H. Camacho, Z. Guan, *J. Am. Chem. Soc.* 129 (2007) 10062–10063.
- [27] H. Liu, W.Z. Zhao, X. Hao, C. Redshaw, W. Huang, W.H. Sun, *Organometallics* 30 (2011) 2418–2424.
- [28] J.L. Rhinehart, L.A. Brown, B.K. Long, *J. Am. Chem. Soc.* 135 (2013) 16316–16319.
- [29] J.L. Rhinehart, N.E. Mitchell, B.K. Long, *ACS Catal.* 4 (2014) 2501–2504.
- [30] S.Y. Dai, X.L. Sui, C.L. Chen, *Angew. Chem. Int. Ed.* 54 (2015) 9948–9953.
- [31] S.Y. Dai, C.L. Chen, *Angew. Chem. Int. Ed.* 55 (2016) 13281–13285.
- [32] L.H. Guo, S.Y. Dai, C.L. Chen, *Polymers* 8 (2016) 37.
- [33] L.H. Guo, C. Zou, S.Y. Dai, C.L. Chen, *Polymers* 9 (2017) 122.
- [34] S.Y. Dai, S.X. Zhou, W. Zhang, C.L. Chen, *Macromolecules* 49 (2016) 8855–8862.
- [35] F.S. Liu, H.B. Hu, Y. Xu, L.H. Guo, S.B. Zai, K.M. Song, H.Y. Gao, L. Zhang, F.M. Zhu, Q. Wu, *Macromolecules* 42 (2009) 7789–7796.
- [36] L.H. Guo, H.Y. Gao, Q.R. Guan, H.B. Hu, J. Deng, J. Liu, F.S. Liu, Q. Wu, *Organometallics* 31 (2012) 6054–6062.
- [37] J. Liu, D. Chen, H. Wu, Z. Xiao, H.Y. Gao, F.M. Zhu, Q. Wu, *Macromolecules* 47 (2014) 3325–3331.
- [38] L. Zhong, G. Li, G. Liang, H.Y. Gao, Q. Wu, *Macromolecules* 50 (2017) 2675–2682.
- [39] D. Pappalardo, M. Mazzeo, S. Antinucci, C. Pellecchia, *Macromolecules* 33 (2000) 9483–9487.
- [40] H. Zou, S. Hu, H.H. Huang, F.M. Zhu, Q. Wu, *Eur. Polym. J.* 43 (2007) 3882–3891.
- [41] A.E. Cherian, J.M. Rose, E.B. Lobkovsky, G.W. Coates, *J. Am. Chem. Soc.* 127 (2005) 13770–13771.
- [42] H.Y. Gao, F.S. Liu, H.B. Hu, F.M. Zhu, Q. Wu, *Chin. J. Polym. Sci.* 31 (2013) 563–573.
- [43] H. Zou, F.M. Zhu, Q. Wu, J.Y. Ai, S.A. Lin, *J. Polym. Sci., Part A: Polym. Chem.* 43 (2005) 1325–1330.
- [44] K.B. Lian, Y. Zhu, W.M. Li, S.Y. Dai, C.L. Chen, *Macromolecules* 50 (2017) 6074–6080.
- [45] R.K. Wang, M.H. Zhao, C.L. Chen, *Polym. Chem.* 7 (2016) 3933–3938.
- [46] X.L. Sui, C.W. Hong, W.M. Pang, C.L. Chen, *Mater. Chem. Front.* 1 (2017) 967–972.
- [47] Z. Feng, R.F. Jordan, *Organometallics* 36 (2017) 2784–2799.
- [48] Z. Feng, J.B. Solomon, R.F. Jordan, *Organometallics* 36 (2017) 1873–1879.
- [49] E.F. McCord, S.J. McLain, L.T.J. Nelson, S.D. Ittel, D. Tempel, C.M. Killian, L.K. Johnson, M. Brookhart, *Macromolecules* 40 (2007) 410–420.
- [50] G. Leone, M. Mauri, F. Bertini, M. Canetti, D. Piovani, G. Ricci, *Macromolecules* 48 (2015) 1304–1312.
- [51] X.X. Wang, L.L. Fan, Y.P. Ma, C.Y. Guo, G.A. Solan, Y. Sun, W.H. Sun, *Polym. Chem.* 8 (2017) 2785–2795.
- [52] K.B. Lian, Y. Zhu, W.M. Li, S.Y. Dai, C.L. Chen, *Macromolecules* 50 (2017) 6074–6080.
- [53] K.S. O'Connor, A. Watts, T. Vaidya, A.M. LaPointe, M.A. Hillmyer, G.W. Coates, *Macromolecules* 49 (2016) 6743–6751.
- [54] X.X. Wang, L.L. Fan, Y.P. Ma, C.Y. Guo, G.A. Solan, Y. Sun, W.H. Sun, *Polym. Chem.* 8 (2017) 2785–2795.
- [55] I. Pierro, G. Zanchin, E. Parisini, J. Martí-Rujas, M. Canetti, G. Ricci, F. Bertini, G. Leone, *Macromolecules* 51 (2018) 801–814.
- [56] G. Leone, M. Mauri, I. Pierro, G. Ricci, M. Canetti, F. Bertini, *Polymer* 100 (2016) 37–44.
- [57] C.S. Popeney, D.H. Camacho, Z. Guan, *J. Am. Chem. Soc.* 129 (2007) 10062–10063.